COMBINED NUMERICAL, FINITE ELEMENT AND EXPERIMENTAL-OPTIMIZATION APPROACH IN THE PRODUCTION PROCESS OF MEDIUM-VOLTAGE, RUBBER-INSULATED ELECTRIC CABLES VULCANIZED WITH STEAM WATER. PART 1: DSC AND RHEOMETER EXPERIMENTAL RESULTS

G. MILANI,[1,*] A. GALANTI,[2] C. CARDELLI,[3] F. MILANI,[4] A. CARDELLI[3]

[1]TECHNICAL UNIVERSITY OF MILAN, PIAZZA LEONARDO DA VINCI 32, 20133, MILAN, ITALY
[2]MIXER COMPOUNDS SPA, VIA CHIARA 6/C 48012, VILLA PRATI DI BAGNACAVALLO (RA), ITALY
[3]IPOOL SRL, RIPA CASTEL TRAETTI 1, 51100 PISTOIA, ITALY
[4]CHEM.CO CONSULTANT, VIA J. F. KENNEDY 2, 45030 OCCHIOBELLO, ROVIGO, ITALY

[*Received May 2015, Revised November 2014*]

INTRODUCTION

The continuous vulcanization (CV) process of cables has been developed more than 50 yr ago. Nevertheless, the use of advanced mathematic studies to predict the performance of polymer compounds is not commonly applied, despite its having an important role in industrial technical development.

In the past few years, high-voltage cables have been produced by using ethylene propylene copolymer and terpolymer EPM/EPDM,[1,2] because of their good dielectric strength, aging resistance,
and partial-discharge resistance. The capability to set up and tune the plant conditions according to cable structure and compound properties has a critical role in cable production and quality.

The use of various types of peroxide and coagents to activate the cross-linking reaction[3–12] is preferred to less-expensive sulfur vulcanization[11] because it leads to well-defined levels of cross-linking of the final product. The level of cross-linking is strictly connected to the final properties of the material, and for this reason, it represents a key parameter in cable production.

The industrial process of cross-linking[3–8] of power cables is usually obtained by means of horizontal (catenary continuous vulcanization [CCV]) systems (Figure 1). In Figure 1, the CCV plant considered in the present article is described.

*Corresponding author. Ph: +39-02-2399-4290; email: gabriele.milani@polimi.it

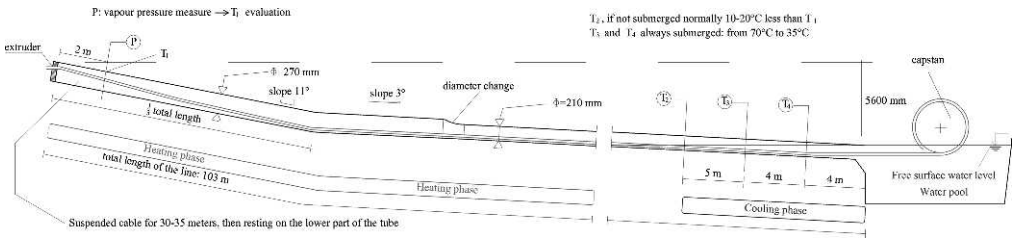

FIG. 1. — Real industrial production line considered.

Peroxide cross-linking is driven by a kinetic law in which both pressure and temperature define the amount of peroxide degradation in radicals. Another parameter to consider is peroxide-radical diffusion in the material matrix.

For these reasons, the changes of process variables associated with the CV line, can cause considerable changes in physical properties, aging characteristics, and heat resistance of the insulation material.[13–15]

Pressure, temperature, and production speed should be kept under severe control to guarantee a designed cross-linking degree. Plant managers can act on both cable linear speed and flooding level of the steam pipe to modify the residence time of the material. Manufacturers usually select the production parameters following their technical experience without any scientific support.

To prevent an undesirable low level of cross-linking of the cable, the authors conducted an experimental campaign cross-linking a medium-voltage electric cable in four different conditions.

Preliminary rheometer characterizations at different temperatures and concentrations of the curing agents were performed to find out the most suitable cross-linking conditions. Several meters of cured samples were produced to measure the cross-linking degree. The level of cross-linking was evaluated through differential scanning calorimetry (DSC), that is, by the content of the unreacted peroxides, on five different radial positions of the cable, from the core to the external layer. Experimental results of the DSC analysis are reported in the article.

The determination of the unreacted quantity of peroxide is not evaluable by the well-known relation between temperature and the half-life ($t_{1/2}$) of peroxide because the curing agent used is a mixture of peroxides. To overtake this limitation, the authors applied a recently proposed, quite-robust kinetic model based on a multiple rheometer characterization, which has been integrated in the thermal analyses.

PEROXIDE CURING PROCESS: KINETIC MODEL FOR PEROXIDE MIXTURES

A detailed, numeric model has been recently proposed by Milani and Milani[9] and Milani and coworkers[16] for a precise characterization of the kinetic behavior of EPDM rubber cross-linked with several peroxides separately or with their particular mixtures. This section provides a numeric assessment of the results obtained experimentally and a brief description of the numeric model used to fit experimental data. The model is based on the kinetics of the reactions occurring in EPDM cured by peroxide through the following steps:

- Translating the chemical reactions into mathematical differential equations (set of first-order, ordinary differential equations [ODE] system);
- Manipulating the ODE system to reduce the problem to a single, nonlinear ODE;
- Solving the nonlinear equation through a standard numeric tool; and
- Estimating the kinetic constants entering into the model with standard least-squares fitting of the experimental rheometer curves.

In this method, the curing process is described as the means of partial reactions occurring in series and in parallel, and their translation into mathematical differential relations constituting an ODE system with many variables, which is typically solved by resorting to numeric methods.

The procedure belongs to an accepted family of numeric approaches that was already tested for the cross-linking of EPDM in presence of peroxides[8,11,16] with some ad-hoc, implemented modifications to adapt the model to the particular study being analyzed.

The fundamental key of the procedure is the evaluation of the kinetic constants for the peroxides mixtures later used to quantify the curing level of medium voltage electric cables. The procedure allows an indirect but reliable estimate of a single kinetic constant describing the whole vulcanization process. Nowadays, these data are available only for pure peroxide and not for mixtures.

The basic chemistry of peroxide curing of EPDM has been reviewed by van Duin and coworkers[17] and could be summarized by the following partial reactions that occur in series and parallel:

$$\begin{gathered}\frac{1}{2}\mathrm{ROOR}\rightarrow \mathrm{RO}\cdot \rightarrow \mathrm{R}'\cdot \quad \text{(initiation)}\\ \mathrm{EP(D)M}-\mathrm{H}+\frac{\mathrm{RO}\cdot}{\mathrm{R}'\cdot}\rightarrow \mathrm{EP(D)M}\cdot +\frac{\mathrm{ROH}}{\mathrm{R}'\mathrm{H}} \quad \text{(H abstraction)}\\ 2\mathrm{EP(D)M}\cdot \rightarrow \mathrm{EP(D)M}-\mathrm{EP(D)M} \quad \text{(combination)}\end{gathered} \tag{1}$$

$$\mathrm{EP(D)M}\cdot +\mathrm{EP(D)M}\rightarrow \mathrm{EP(D)M}-\mathrm{EP(D)M}\cdot \rightarrow \mathrm{EP(D)M}-\mathrm{EP(D)M}-\mathrm{H} \quad \text{(addition)}$$

where M–H in Eq. 1 is a bond between hydrogen and a carbon belonging to the backbone of the macromolecules

The chain of free-radical reactions starts by thermal decomposition of the peroxide, yielding primary alkoxy (RO·) or secondary alkyl radicals (R·).

Subsequent abstraction of H-atoms from the EPDM polymer results in the formation of EPDM macroradicals (EPDM·). Calculations based on kinetic data for H-abstraction indicate that H-abstraction mainly occurs along the saturated EPM polymer backbone, whereas several electron paramagnetic resonance (EPR) spectroscopy studies have shown the selective formation of allyl radicals derived from the diene monomer.

Considering the energy required for the abstraction of the H-atoms within the formation of the backbone, the allyl radicals are more probable than the others because of the lowest energy required by the abstraction of the H-atoms.

The EPDM cross-linking proceeds via two additive pathways: one EPDM macroradical could combine with another macroradical or, alternatively, react with an EPDM unsaturation. Visible spectroscopy has confirmed the conversion of the EPDM unsaturation upon peroxide cure.

EPDM–peroxide compounds coagents, such as triallyl isocyanurate, trimethylolpropane trimethacrylate, or *m*-phenylenebis(maleimide), are used to increase the peroxide curing efficiency affecting the mechanism of peroxide cure.

In the numeric model, we adopted the kinetic scheme for the peroxide cross-link reactions summarized in Eq. 1 because it reproduces the most important steps occurring during peroxide curing and is simple to handle.

The polymerization scheme obtained in translating the chemical reactions in Eq. 1 in a mathematical framework, and focusing exclusively on EPDM rubber, uses the following reactions:

$$I \xrightarrow{K_1} 2R \qquad R+P \xrightarrow{K_2} P^* \qquad 2P^* \xrightarrow{K_3} P_r^* \qquad P^* \xrightarrow{K_4} P^* \tag{2}$$

In Eq. 2, I is the peroxide; R is the primary alkoxy (RO·) or the secondary alkyl radicals (R·); P is the uncured polymer; P^* is the EPDM macroradical; P_r^* and P^* are the matured, cross-linked polymers, respectively; and $K_{1,\ldots,4}$ are the kinetic reaction constants. Here, $K_{1,\ldots,4}$ are temperature-dependent quantities; hence, they should rigorously be indicated as $K_{1,\ldots,4}(T)$, where T is the absolute temperature.

Temperature dependence will be ignored in following steps to simplify the calculation.

Polymer concentration (P) versus time (t) can be estimated using *xyz* method after suitable mathematical manipulation:

$$\frac{d^2P}{dt^2} - \frac{1}{P}\left(\frac{dP}{dt}\right)^2 + K_2P\frac{dP}{dt} + 2K_1K_2I_0P\,\exp[-K_1(t-t_o)] = 0 \tag{3}$$

Further details on Eq. 3 derivation could be found in ref 9.

The nonlinear differential Eq. 3 may be solved numerically with a standard Runge–Kutta algorithm to find concentration $P(t)$.

The knowledge of $P(t)$ allows the determination of quantity $R(t)$ and P^* (see ref 9):

$$\frac{dP^*}{dt} = K_2R(t)P(t) - K_3(P^*)^2 - K_4P^* \tag{4}$$

Equation 4 is again solved using a Runge–Kutta numeric approach.

The combined application of Eqs. 3 and 4 with least-squares minimization allows an estimation of the kinetic constants entering into the reaction scheme in Eq. 2, assuming the experimental rheometer curves as the target. The experimental cure values should be normalized, dividing each point of the curve by the maximum torque values to perform a numeric optimization of the proposed kinetic model.

The entity of experimental campaigns could be significantly reduced by applying the model proposed and verified in refs 8 and 16. An innovative software has been developed by using numeric prediction and implementation of the mathematical kinetic model to set up temperature profiles of the CV line.

DETERMINATION OF TEMPERATURE PROFILES IN THE VULCANIZATION TUBE

A short overview of the mathematical basis of the numeric approach employed for the determination of cable-temperature profiles under curing is reported. The production line is supposed to be constituted by a vulcanization pipe (with water steam at high temperatures), followed by a water cooling phase (at lower temperature), as reported in Figure 1.

Steam temperature adopted by manufacturers usually depends on the peroxide employed for the EPDM cross-linking. Linear speed of the cable determines the exposition time at a fixed pipe length. At a given exposition time, the temperature cross-linking degree of each layer can be numerically estimated by applying standard heat-transmission physical laws.

The analyses conducted hereafter refer to a real CV line. Its basic scheme is sketched in Figure 1. The head of the extruder is connected to the vulcanization pipe. After extrusion, the cable passes into a pipe containing water steam under pressure. Finally, the tube is connected with submerged equipment in cooling water. The linear speed of the cable is controlled by the capstan at the end of the line.

The CV pipe considered in this work is 103 m long and exhibits an initial inclination of 11° for approximately one-third of its length. After this zone, the pipe shows a slight residual slope of 3°. The diameter of the pipe is initially equal to 270 mm and is reduced to 210 mm starting at one-half of its length.

TABLE I
EXPERIMENTAL DATA SET ANALYZED, EPDM COMPOSITION IN GRAMS

Polymer[a]	100
Silane treated calcinated kaolin	55.5
Antioxidants	14.8
LDPE Riblene MR 10 MFI= 18.7 (ASTM Standard D 1238)	11.1
PE WAX	1.8
Peroxide mixture M3	1.1

[a] Vistalon 1703P; ethylene in weight by percentage: 76.2; VNB, vinylnorbornene, in weight by percentage: 0.9%; Mooney ML (1 + 4), 100 °C 35.3; Manufacturer: ExxonMobil.

An Analogic (Wakefield, MA, USA) manometer is located 2 m after the head of the extruder and is used to measure the steam pressure during the vulcanization process. In the last 15 m of the pipe, the cable is cooled by a water pool at 35°–40°C. The capstan is also partially submerged. If the free surface of the water in the pool is considered as reference, the depth of the extruder head is equal to 5.6 m. In the initial part, the cable is suspended inside the pipe, but after 30–35 m, it rests on the lower part of the vulcanization device because of the combined action of gravity and slope change, posing doubts about the effective, symmetric cross-linking of the item under such physical conditions. Because the cable enters into the last portion of the line in correspondence with the lower part of the pipe, it immediately meets the cooling water pool. Therefore, the water level has to be checked with particular care so it does not vary significantly throughout the length of the heating zone.

Three thermometers are placed in the last 15 m, at mutual distances of 4–5 m, and are labeled in Figure 1 as T_2, T_3, and T_4, respectively. Theoretically, T_2 should measure the same temperature deduced from the pressure measurement at the beginning of the line (i.e., T_1), but, in practice, this never occurs because T_2 is usually 10–20 °C lower than T_1 is, near the surface of the water. This issue depends intrinsically on the design of the plant and partially on the initial temperature imposed. In some cases, the T_2 section is submerged with no temperature check at the end of the heating phase. No thermometer probes are installed in intermediate position, from the beginning to the end of the heating phase. T_3 and T_4 thermometers monitor the temperature of the water pool.

The experimental campaign was conducted under the following four different cross-linking conditions:

- Test 1: Temperature $T_1 = 202$ °C; total curing time $t_c = 5.6$ min
- Test 2: Temperature $T_1 = 212$ °C, total curing time $t_c = 5.6$ min
- Test 3: Temperature $T_1 = 202$ °C, total curing time $t_c = 7.7$ min
- Test 4: Temperature $T_1 = 212$ °C, total curing time $t_c = 7.7$ min

EXPERIMENTAL RHEOMETER CURVES: KINETIC MODEL PERFORMANCE (DETERMINATION OF REACTION KINETIC CONSTANTS) AND FINAL MECHANICAL PROPERTIES

The polymer used was a commercial EPDM, with properties furnished by the provider and summarized in Tables I and II. In Table II, two other commercial products are considered for comparison purposes.

A preliminary characterization of the molecular-weight distribution was conducted in the laboratory (Figure 2). Molecular weight is reported in the horizontal axis (logarithmic scale),

TABLE II
CHARACTERISTICS OF THE POLYMERS CONSIDERED IN FIGURE 2

Type of polymer	ML (1 + 4) Mooney viscosity 100 °C	ML (1 + 4) Mooney viscosity 125 °C	% Ethylene by wt	% VNB by wt	Molecular weight distribution (Figure 1)
Vistalon 1703 by Exxon	—	25	77	0.9	Very broad
Vistalon 785 by Exxon	—	30	49.0	—	Narrow
Dutral CO-058 by Polimeri Europa	80	—	52	—	Narrow

whereas, in the vertical axis, the normalized differential-weight fraction is reported in arbitrary units. The area bounded by the curve, the x-axis, and a fixed molecular weight (M_{w0}) divided by the total area under the curve, represents the probability of finding molecular weights less than M_{w0}. A critical comparison among all the curves shows that the Vistalon 1703 (ExxonMobil Chemical Company, Spring, TX, USA) molecular weight distribution is wider than other commercial products available.

The other row materials used to produce the EPDM compound include the following:

- Silane-treated, calcinated kaolin, Polarite 503S, provided by Imerys (Paris)
- Low-density polyethylene, Riblene MR10, supplied by Polimeri Europa (Eni, Rome) (density, 0.918; melt flow rate, 190 °C/2.16 Kg 20 g/10 min)
- PE Wax A-C 617A, provided by Honeywell (Morristown, NJ, USA) (drop point, 101 °C).
- Antioxidant polymerized 2,2,4-trimethyl-1,2-dihydroquinoline, provided by LanXess (Cologne, Germany).

The mixture (M3) of peroxides used as curing agent was a composition of three different peroxides: Trigonox T, Perkadox BC-FF, and Perkadox 14S (AkzoNobel, Amsterdam, the

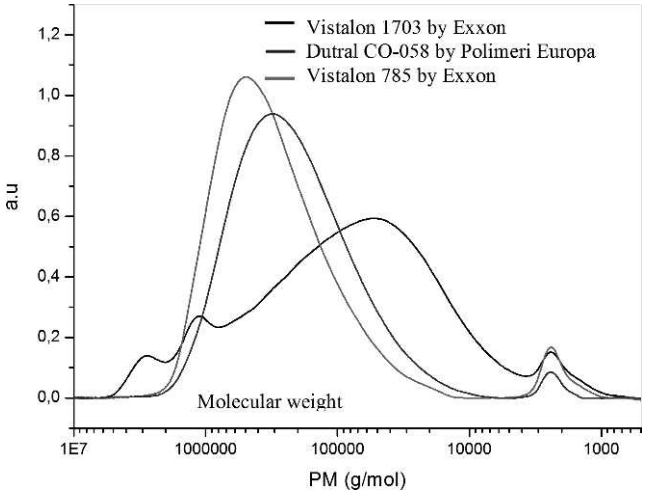

FIG. 2. — Molecular weight distribution of Vistalon 1703 compared with the distributions of two other common industrial products.

TABLE III
HALF-LIFE TEMPERATURES OF THE PEROXIDES ANALYZED AT 0.1, 1, AND 10 H

Peroxide typology[a,b]	$t_{1/2}$ in hours		
	0.1	1	10
Trigonox T	169	146	117
Perkadox BC-FF	162	138	112
Perkadox 14 S-FL	169	146	117

[a] Trigonox T, *ter*-butylcumylperoxide; Perkadox BC-FF, dicumyl peroxide; Perkadox 14S-FF, di(*tert*-butylperoxyisopropyl) benzene.
[b] Curing agent M3 is a mixture of BC-FF, 14S-FF, and Trigonox T.

Netherlands). As reported in Table III, M3 was constituted by two commercial peroxides with the same thermal decomposition constants.

For the composition and to use of the M3 mixture of peroxides, the reader is referred to ref 16.

To evaluate the optimal concentration of M3, the mixture was added to the EPDM compound using a laboratory twin-roll mixer at a temperature of 85 °C. The peroxide was added to the melted compound, and then, the blend was homogenized for 10 min.

A precise insight of (1) the optimal M3 concentration, and (2) a prediction of the behavior under different temperature conditions, was required to estimate the kinetic-reaction constants to be used within the mathematical model.[16] For this reason, a wide experimental characterization on five different molar concentrations and curing temperatures was conducted by the authors.

The amount of peroxide, referred to as "100 g of polymer," is variable. The chosen standard concentration, labeled as "±0%", is equal to 5.037 mmoles/100 g of polymer. It was considered a "reference" because that is the concentration used in standard industrial production of the compound.

Four additional concentrations were tested, called −50%, +50%, +100%, and +150%. Labels indicate the molar concentration of the curing agent with respect to the standard concentration. For instance, a +50% concentration indicates that 1.5 mol, with respect to the standard, was used.

Three different vulcanization temperatures where inspected, typical for the curing of medium- to high-voltage electric cables, namely 160 °C, 180 °C, and 200 °C.

DSC analysis was used to quantify the unreacted, cross-linking agents,[18] and rheometer curves were used to obtain indirect information on the state of the cure, or the cure efficiency, of the cross-linking agent, as extensively demonstrated by Sun and Isayev.[19] The average $M(t)$ curves obtained may indeed be used to calculate the evolution of the cross-linking degree $\alpha_{\exp(t)}$ using the Sun and Isayev[19] relation:

$$\alpha_{\exp(t)} = \frac{M(t) - M_{\min T}}{M_{\max T_0} - M_{\min T_0}} \tag{5}$$

where (1) $M_{\min\ T}$ is the minimum value of torque S′ during a cure experiment at temperature T. Before reaching this minimum value, $\alpha_{\exp}$ is considered equal to zero, and (2) $M_{\min T_0}$ and $M_{\max T_0}$ are the minimum and maximum torque values, obtained for a cure experiment at a temperature T_0 low enough to allow neglecting reversion. In this way, the rheometer curves to fit always range between 0 and 1, with a maximum torque sensibly less than 1 for high-temperature vulcanizations.

Experimental results rely on thermal characterizations to determine the state of the cure of each sample, conducted with a standard oscillating disc rheometer (ODR), and their mechanical characterizations, particularly for tear and tensile-strength tests.

The state of cure for each sample was obtained using an ODR (GB3 RheoCheck, Gibitre Instruments, Bergamo, Italy), whereas final characterization was obtained with a tensile tester (GB3 TensorCheck, Gibitre Instruments).

ODR tests were conducted following ASTM Standard D 2084-81.[20] Samples were prepared in agreement with ASTM Standard D 1485 (ref 21) method for small, cylindrical specimens with a diameter equal to 20 mm and a height equal to approximately 12.5 mm. Specimens were conditioned at constant room temperature equal to 25 °C. Three different temperatures at five different concentrations were studied, each one replicated three times, obtaining 45 rheometer curves experimentally determined. Reported results refer to mean values obtained among replicates.

Cross-linked samples at the different temperatures and concentrations were mechanically tested to determine tensile strength, elongation at break, and tear resistance. The samples for mechanical tests were molded under 50-bar pressure and maintained for a time equal to compound t_{90}, previously deduced from the rheometric curves. Samples were prepared according to ASTM Standard D 1456-86.[22] A huge amount of thermal and mechanical data were thus collected and postprocessed, as summarized below.

RHEOMETER CURVES AND MECHANICAL CHARACTERIZATION EXPERIMENTAL RESULTS

In Figures 3 and 4, ODR results (mean values of three replicates) for concentrations equal to –50%, ±0%, 50% set and 100%, 150% set are reported, respectively. In Figure 5, normalized rheometer curves obtained at the three different temperatures (Figure 5a: 160 °C, Figure 5b: 180 °C, and Figure 5c: 200 °C) are depicted for all the concentrations inspected. The curves refer to the different concentrations explored in the experimental campaign, namely –50%, ±0%, +50%, +100%, and +150%. They exhibit a maximum torque close to 55 dNm, which lessens at lower concentrations (especially at –50%), whereas a concentration increase results in a beneficial effect.

The absence of reversion (a decrease of torque after reaching the maximum) and the homogeneity of minimum and maximum values of torque at the three temperatures allow a normalization of the analysis simply by dividing each value of the torque by the maximum torque[9] measured during the test. For the cases where a reversion is present, the reader is referred to Milani and Milani.[23]

Experimental evidence showed that a maximum cross-linking density could be obtained with at double amount of peroxide in comparison to the standard one (+100% concentration).

Rheometer curves tend asymptotically to that corresponding to a concentration equal to 150%. This means a further increase in peroxide concentration would not drive an increase in the final cross-linking density.

Kinetic constants of the M3 mixture are evaluated numerically with the kinetic model previously discussed. Numerically predicted rheometer curves resulting from the fitting process are depicted and compared with experimental ones in Figure 6 (Figure 6a: 160 °C, Figure 6b: 180 °C, and Figure 6c: 200 °C). The numeric fitting overlaps almost perfectly with the experimental curves, validating the kinetic constants related to the reaction scheme in Eq. 1 assumed for the calculations.

Numeric curves were obtained using a nonlinear least-squares procedure. Figure 7 shows the difference between normalized, experimental torque and numeric predictions at successive iterations and between the initial and final time of experimentation. As expected, the difference decreases drastically passing from the initial iteration to the final point, meaning that the least-squares routine is achieving convergence. The gap between numeric models and the experimental data tends toward zero for most instances inspected, except the initial simulation range near the scorch point. In that point, the experimental curve exhibits a sudden increase in the first derivate, meaning that cross-linking is prone to occur. That stage has little relevance for the proposed models

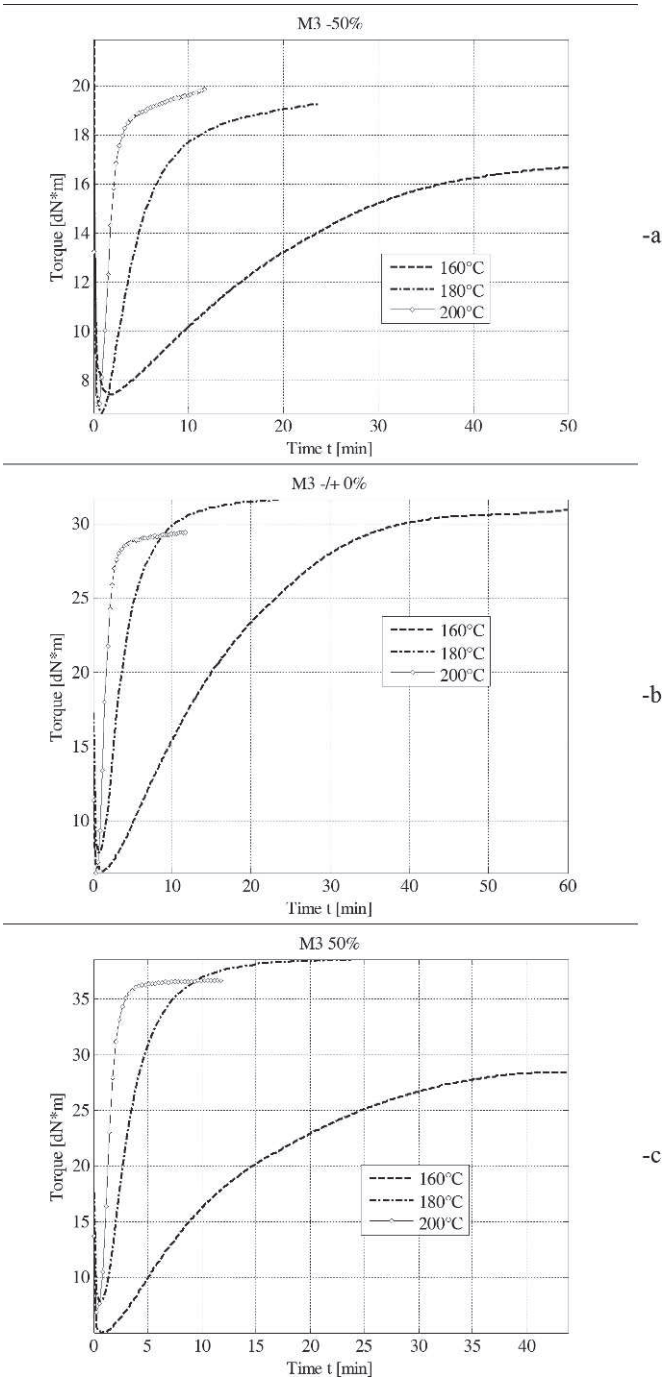

FIG. 3. — M3 curing agent. Experimentally obtained rheometer curves (mean values from three replicates). (a) –50%. (b) ± 0%. (c) 50%.

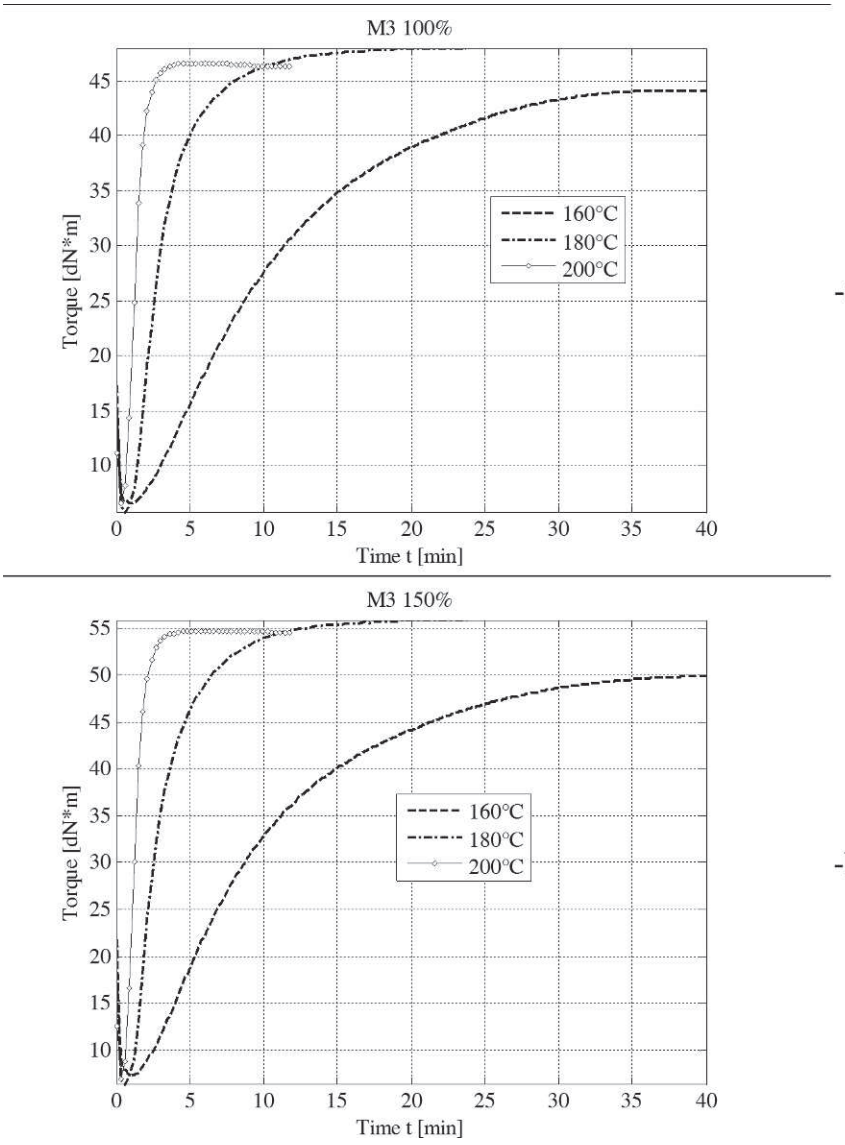

FIG. 4. — M3 curing agent. Experimentally obtained rheometer curves (mean values from three replicates). (a) 100%. (b) 150%.

because the model was designed for a reliable prediction of the final reticulation level. As extensively demonstrated in refs 9 and 24, the fitting of the experimental response is satisfactory, as shown by superposition of the calculated curves with experimental data.

Considering the numeric values obtained for the two constants K_1 and K_2 at three distinct temperatures (the other constants, K_3 and K_4, are close to zero, indicating that no reversion was experienced), the lines passing from such values in the Arrhenius plane were plotted. In this space, the horizontal axis is represented by the inverse of the absolute temperature, $1/T$, whereas the vertical axis is $\log(K_i)$, where K_i is the ith kinetic constant. This means that variability of a single kinetic constant follows the so-called Arrhenius law described as $K_i(T) = K_{i0} \exp[(E_{ai})/(R_g T)]$,

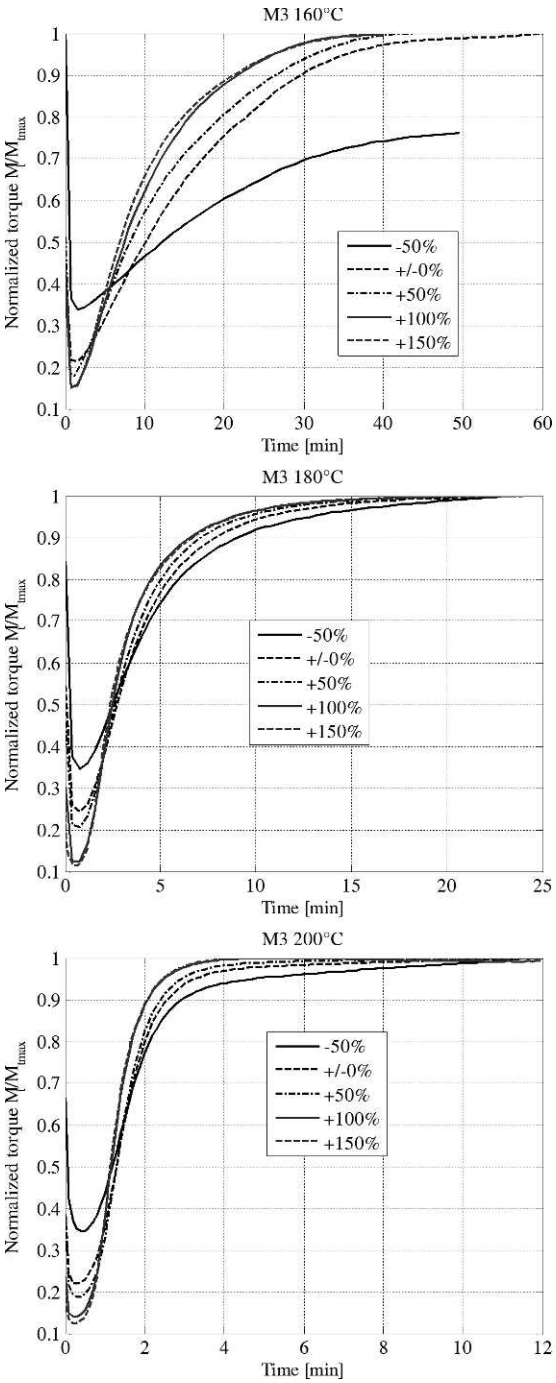

FIG. 5. — M3 peroxides mixture. Normalized, experimental rheometer curves at different peroxide concentrations. (a) 160 °C. (b) 180 °C. (c) 200 °C.

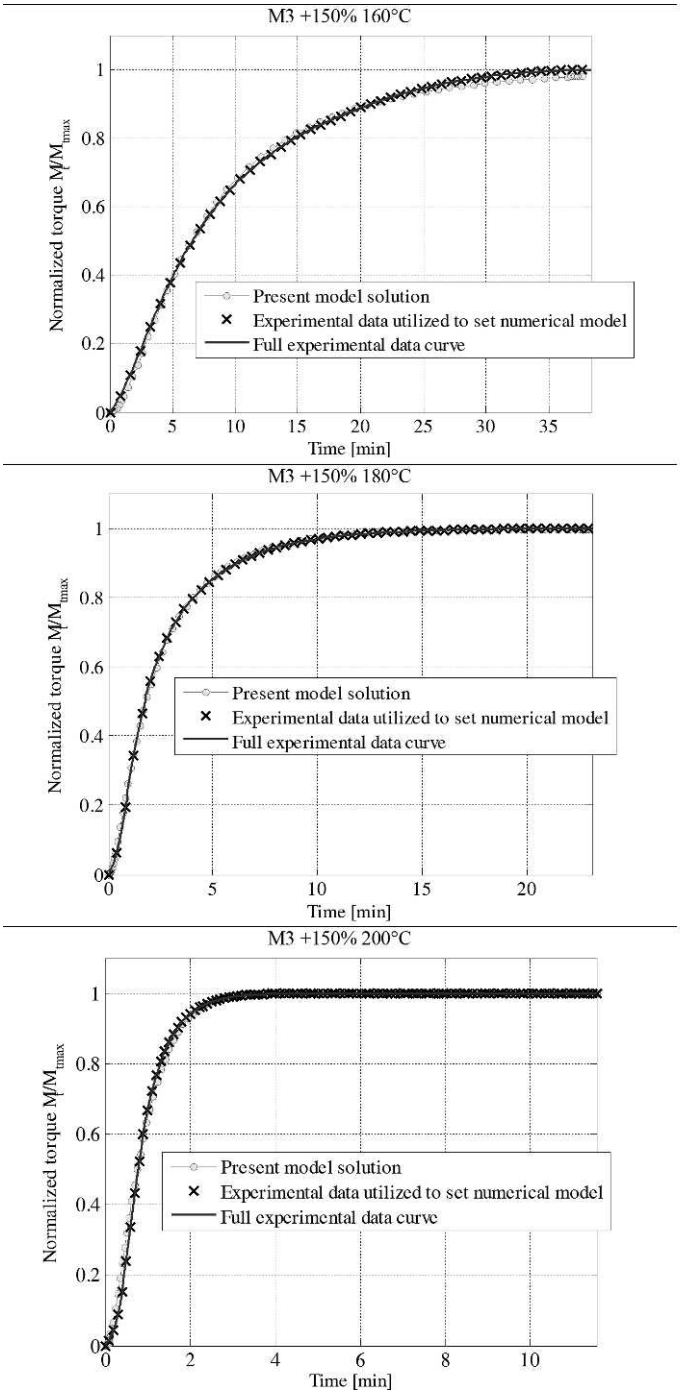

FIG. 6. — M3 curing agent. Comparison between normalized, experimental rheometer curve and numeric model predictions. (a) 160 °C. (b) 180 °C. (c) 200° C.

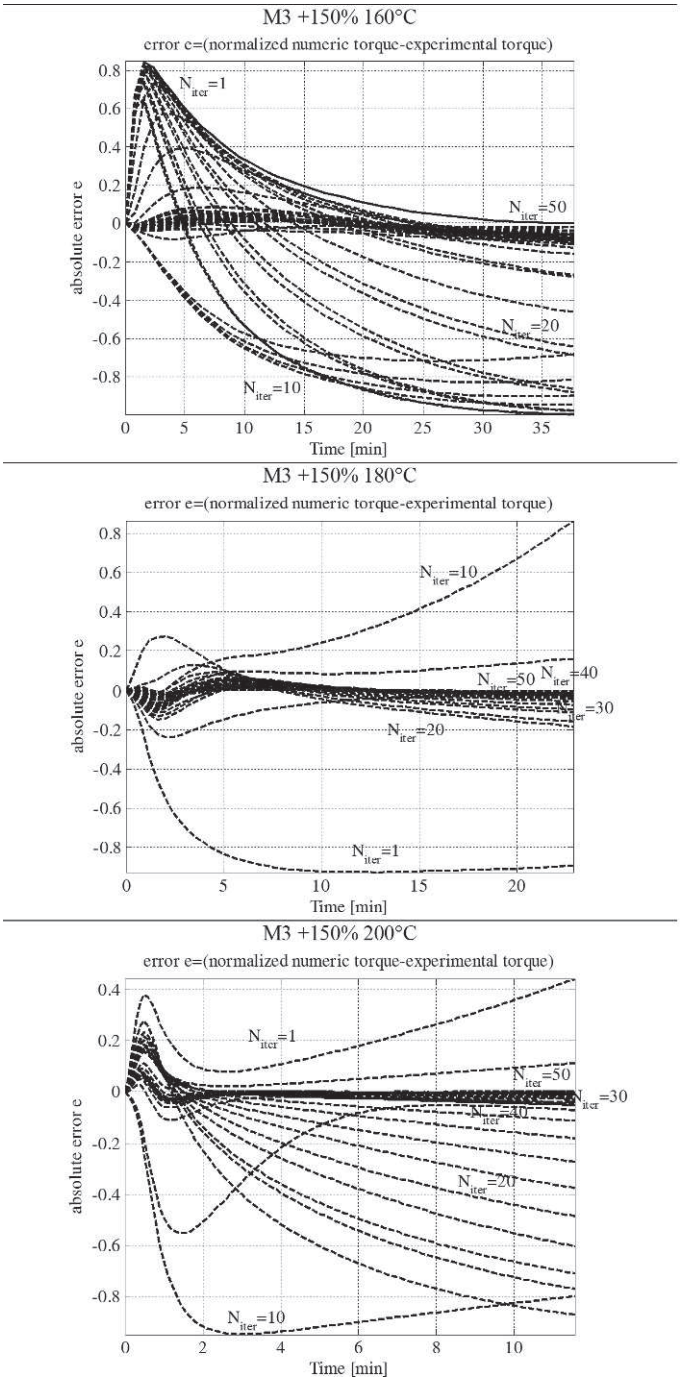

FIG. 7. — M3 curing agent. Difference between numeric model and experimental, normalized torque at successive iterations. (a) 160 °C. (b) 180 °C. (c) 200 °C.

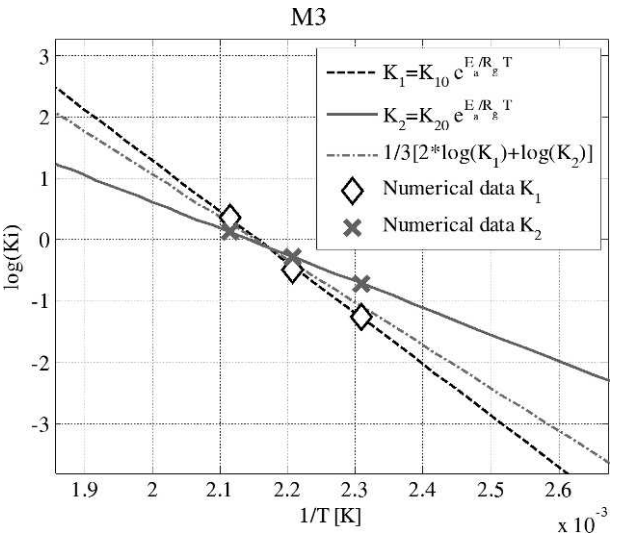

FIG. 8. — Linear regression interpolation of the kinetic constants K_1 and K_2 provided by the single differential-equation model and the resultant linear regression obtained as weighted sum of K_1 and K_2.

where K_{i0} is the value of the ith kinetic constant at an infinite temperature, E_{ai} is a constant typical of the reaction, and R_g is the universal gas constant. In a $1/T - \log(K_i)$ Cartesian plane, the Arrhenius law is represented by a line intercepting vertical axis at $\log(K_{i0})$. Using experimental data collected at two distinct temperatures and accepting that each single constant follows the Arrhenius law, it is possible to sketch $K_i(T)$ lines in the $1/T - \log(K_i)$ plane for the peroxides studied. The calculated lines are plotted in Figure 8. In ref 16, it was shown that numeric results may be compared with

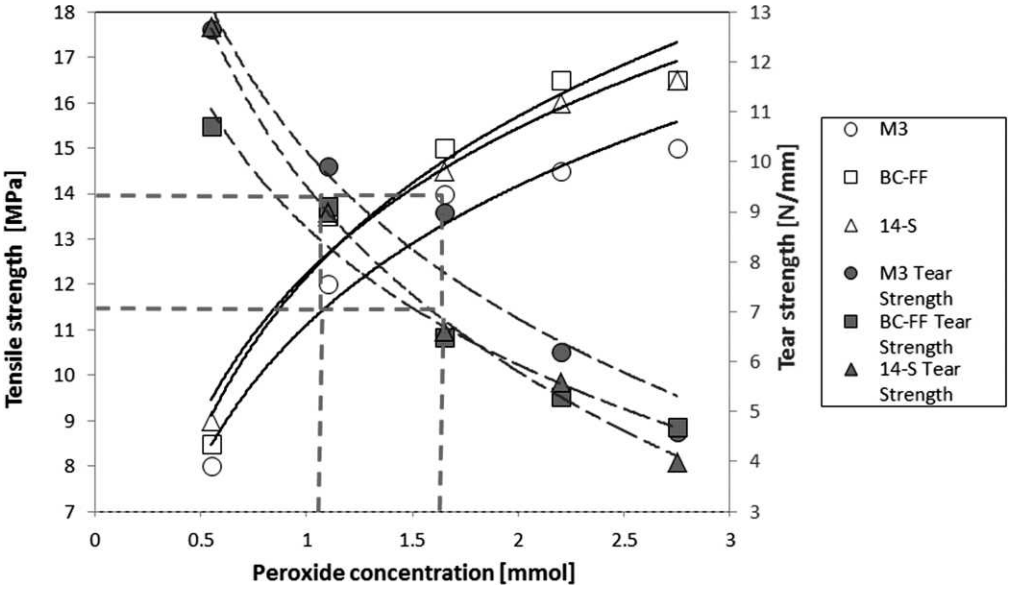

FIG. 9. — Peroxide concentration vs tear strength and tensile strength obtained with different peroxides and with a peroxide mixture.

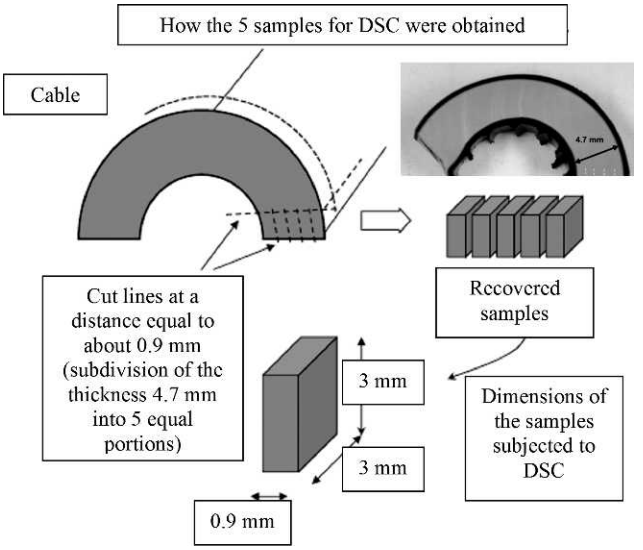

FIG. 10. — DSC sample preparation starting from cables.

available commercial data, when a single peroxide is considered. For mixtures of peroxides, a weighted average between constants K_1 and K_2 should be considered, plotting the line as $1/3 \times (2 \log K_1 + \log K_2)$. An accurate fitting (the dash-dot line in Figure 8) is deduced from the numeric results of single peroxides, validating the suggested approach.

The results of the mechanical characterization tests are synthesized by the diagram in Figure 9. The diagram contains a double-vertical axis referring to the experimental values of tensile strength and tear strength. Both of them are plotted as a function of the peroxide concentration in the compound. Results obtained for M3 were compared with those resulting from a standard cross-linking conducted using two commercial peroxides as cross-linking agents: Perkadox BC-FF (BC-FF) dycumil peroxide and Perkadox 14S-FL (14S) di(*tert*-butylperoxyisopropyl) benzene.

A numeric interpolation of the experimental data is provided to summarize the trends in the analysis:

1. By increasing the reticulation-agent concentration, the tensile strength increases and the tear-resistance decreases;
2. BC-FF provides high tensile-strength values but lower values of tear resistance; and
3. M3 provides an optimal ratio between tensile strength and tear resistance for all concentrations tested.

Therefore, the M3 mixture provides the best compromise between maximum efficiency in tensile and tear strength (see Figure 9).

EXPERIMENTALLY DETERMINED DEGREE OF CROSS-LINKING

The DSC has become the most-used thermal analyzing technique. We have used this technique to quantify the vulcanization degree[25] and, hence, the unreacted peroxide after the cross-linking process, recovering samples across the sample section, according the procedure envisaged in Figure 10.

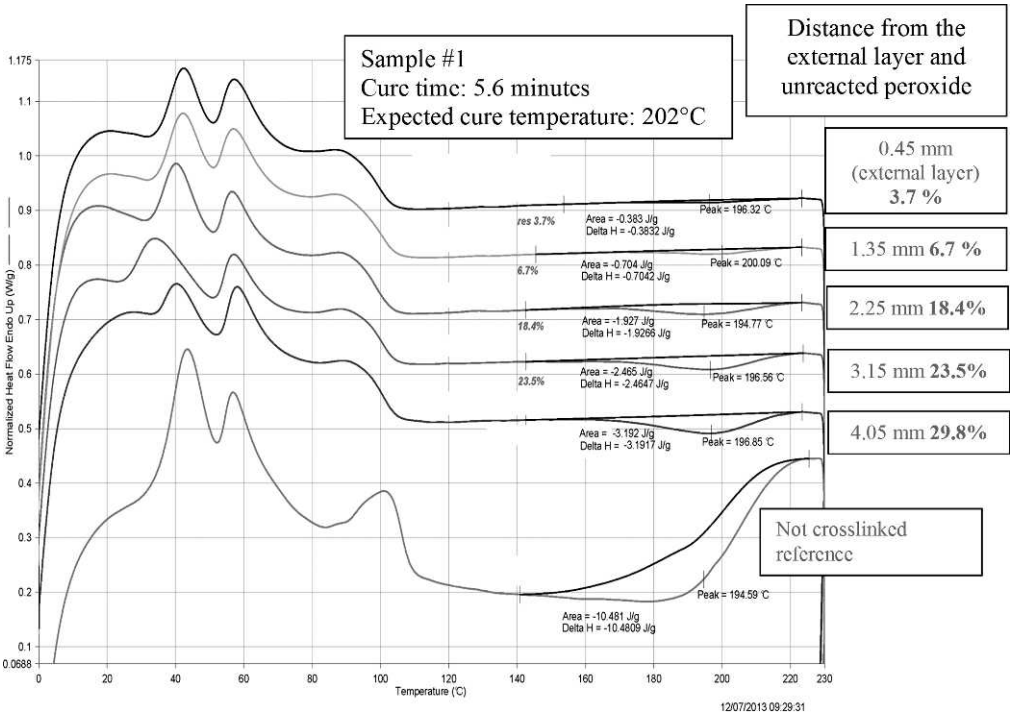

FIG. 11. — Sample 1: DSCs from different positions in the external layer compared with the DSC of the sample that was not cross-linked.

DSC measurements were carried out by using a PerkinElmer (Waltham, MA, USA) DSC 6000. To verify the profile of the cross-linking degree on the cable insulation, five samples were cut at 1 mm increments along the cross-section (0.9 mm external surface, 1.8, 2.7, 3.6, and 4.7 mm internal surface, as reported in Figure 10). The analyses were carried out on 10–15 mg samples in the temperature range from 0 to 230 °C at the scanning rate of 20 °C/min under inert atmosphere (N_2) in punched aluminum pans.

The heat released during the curing reaction (ΔH), calculated from the exothermic peak with a maximum around 195 °C, can be considered directly proportional to the cross-linking residue. The residual heat of reaction (ΔH_r) found in each section is a direct measure of the cross-linking degree because the residue depends on the unreacted peroxide. The residual, unreacted peroxide was calculated to evaluate the cross-linking degree using the following equation:

$$\text{Residue} = \frac{\Delta Hr}{\Delta H_0} \tag{6}$$

where ΔH_r refers to the peroxide in the sample, and ΔH_0 refers to the peroxide in the compound that was not cross-linked and is used as a reference (100% of the cross-linking residue).

Figures 11–14 show the results of the DSC performed for the above test conditions with the corresponding evaluation of the unreacted peroxide concentration. In each figure, six curves are shown. Five curves refer to the different positions across the cable section, whereas the last curve is the reference for the sample before cross-linking. The representation refers to the normalized heat flow measured plotted against temperature.

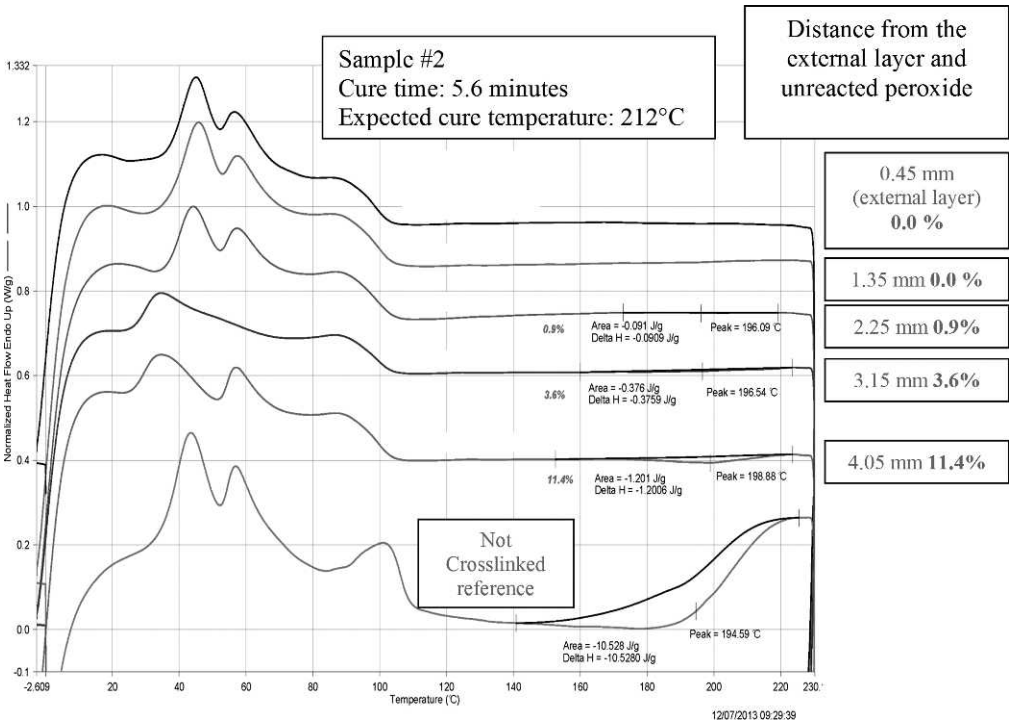

FIG. 12. — Sample 2: DSCs from different positions in the external layer compared with the DSC of the not cross-linked sample.

Residual values of peroxide are collected in Tables IV and V, where the results of the DSC experimental campaign are synoptically represented.

CONCLUSIONS

The experimental study on the CV line, cross-linked EPDM allowed us to draw the following conclusions:

1. Optimization of final mechanical properties can be obtained with a detailed mechanical characterization at different curing-agent concentrations; and
2. A mixture of peroxides reduces the gap between tensile and tear strength performances.

DSCs and classical rheometric curves are key tools for double-checking the unreacted peroxide concentration and the efficiency of the curing agent used.

TABLE IV
EXPERIMENTALLY DETERMINED QUANTITY OF UNREACTED PEROXIDE, TESTS 1 AND 3, AT A TEMPERATURE OF 202 °C

	Distance from the surface (mm)				
Curing time (min)	0.9	1.8	2.7	3.6	4.7
5.6 (test 1)	3.7	6.7	18.4	23.5	29.8
7.7 (test 3)	0	0	0.2	2.1	3.7

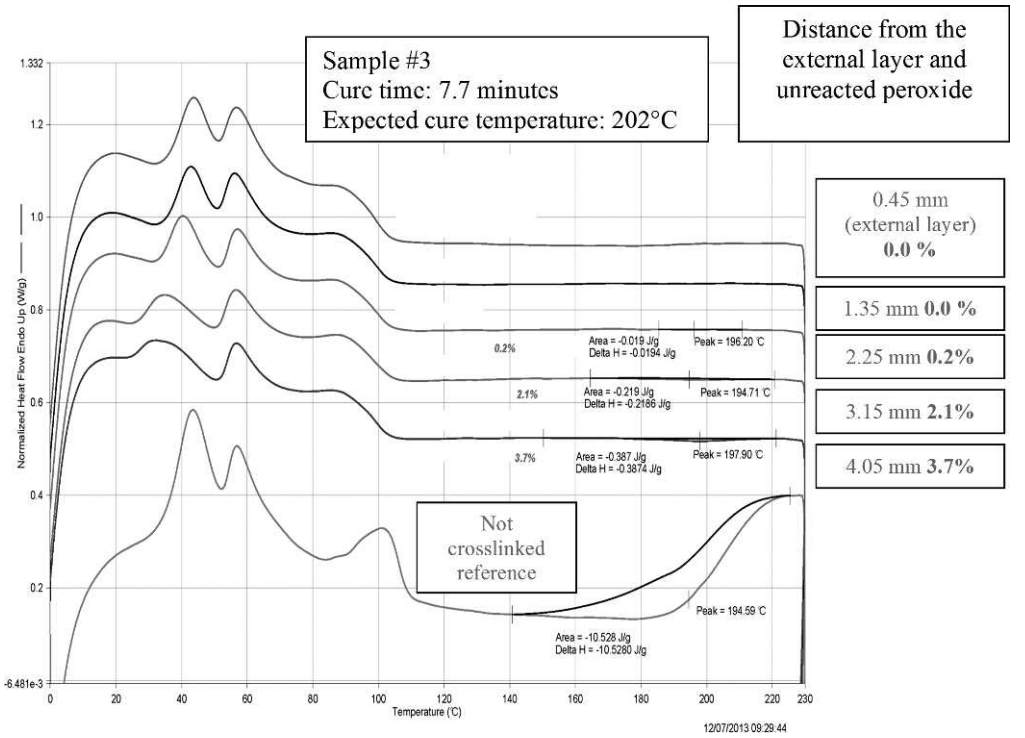

FIG. 13. — Sample 3: DSCs from different positions in the external layer compared with the DSC of the sample that was not cross-linked.

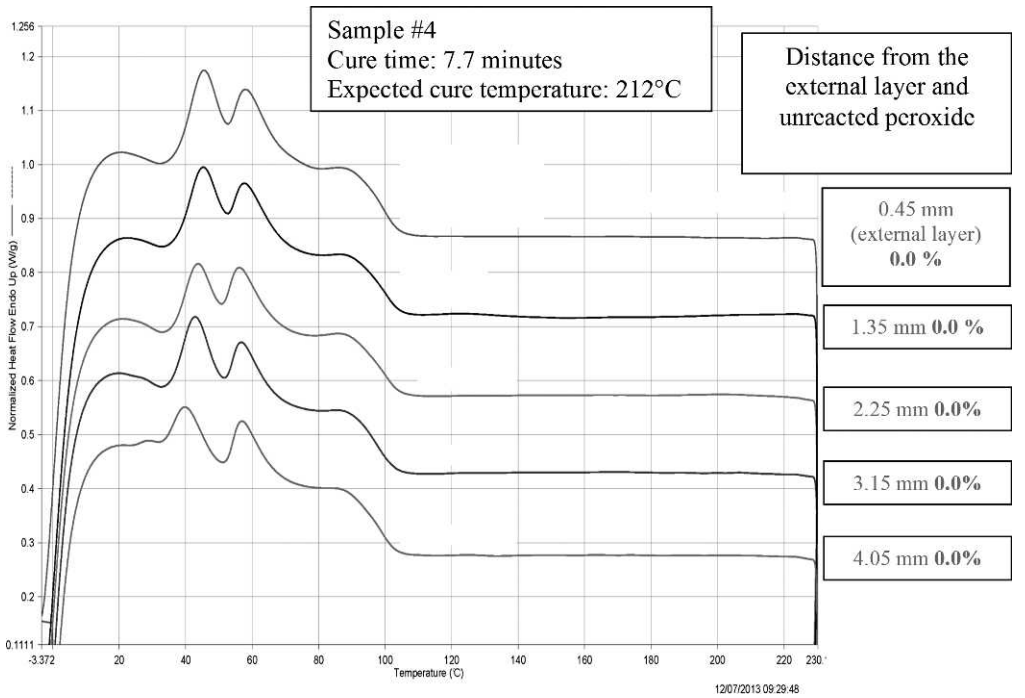

FIG. 14. — Sample 4: DSCs from different positions in the external layer compared with the DSC of the sample that was not cross-linked.

TABLE V
EXPERIMENTALLY DETERMINED QUANTITY OF UNREACTED PEROXIDE, TESTS 2 AND 4, AT A TEMPERATURE OF 212 °C

	Distance from the surface (mm)				
Curing time (min)	0.9	1.8	2.7	3.6	4.7
5.6 (test 2)	0	0	0.9	3.6	11.4
7.7 (test 4)	0	0	0	0	0

An experimental correlation between tensile strength and tear strength at four different curing conditions was found by varying the concentrations of the curing agent.

To explain the intuitively wrong experimental result, we suggest the vapor condenses and generates a temperature drop that is ignored industrially because of the absence of specific monitoring systems for pressure and temperature along the pipe. A complete system controlling steam pressure should be installed to guarantee a constant and well-defined temperature along the whole length of the plant and to precisely determine where the temperature–pressure couple is located in the vapor–liquid equilibrium system.

The accompanying article (Part 2; in press) presents a comprehensive numerical investigation, based on the kinetic mathematical approach presented here, coupled with finite-element computations, and applied to the experimental case discussed here, assuming in the numerical model that there is a drop in steam temperature along the length of the pipe, to minimize the error between experimentally obtained data and numerically predicted output.

REFERENCES

[1]F. P. Baldwin and G. Ver Strate, RUBBER CHEM. TECHNOL. **45**, 709 (1972).

[2]R. H. Schwarr and C. H. Chien, *Ethylene-Propylene CO and TER polymer Rubber, Report 4b*, Stanford Research Institute, Menlo Park, CA, 1981.

[3]D. C. Seymour and D. Krick, *J. Elastomers Plast*. **11**, 97 (1979).

[4]R. C. Milner, *Wire* **23**, 271 (1973).

[5]B. E. Roberts and S. Verne, *Plast. Rub. Proc. Appl*. **4**, 135 (1984).

[6]R. E. Drake, J. J. Holliday, and M. S. Costello, *Rubber World* **213**, 22 (1995).

[7]L. Palys, J. Brennan, F. Debaud, L. Keromnes, and A. Defrancisci, "Improved Processability and Productivity of Wire and Cable Compounds Using SP2 Scorch Protected Organic Peroxides," *56th IWCS Conference*, Proceedings of the International Wire and Cable Symposium, Inc., Lake Buena Vista, FL, November 11–14, 2007, IWCS, Shrewsbury, PA, 2007, pp. 594–601.

[8]G. Milani and F. Milani, *Comput. Chem. Eng*. **32**, 3198 (2008).

[9]G. Milani and F. Milani, *J. Math. Chem*. **51**, 1116 (2013).

[10]P. R. Dluzneski, RUBBER CHEM. TECHNOL. **74**, 451 (2001).

[11]G. Milani and F. Milani, *Polym. Eng. Sci*. **53**, 353 (2013).

[12]L. D. Loan, RUBBER CHEM. TECHNOL. **40**, 149 (1967).

[13]V. Kozar and Z. Gomzi, *Thermochim. Acta* **457**, 70 (2007).

[14]V. L. Lenir, *Polym. Eng. Sci*. **24**, 633 (1984).

[15]S. D. Gehman, RUBBER CHEM. TECHNOL. **40**, 36 (1967).

[16]G. Milani, A. Galanti, C. Cardelli, and F. Milani, *J. Appl. Polym. Sci*. **131**, 40075 (2014).

[17]M. van Duin, *Kautsch. Gummi Kunstst*. **55**, 150 (2002).

[18]H. H. Willard, L. L. Merritt, Jr., J. A. Dean, and F. A. Settle, Jr., "Thermal Analyses," in *Instrumental Methods of Analysis*, 7th ed., Wadsworth Publishing Company, Belmont, CA, 1988.

[19]X. Sun and A. I. Isayev, RUBBER CHEM. TECHNOL. **82**, 149 (2009).

[20]ASTM Standard D 2084-81, "Standard Testing Method for Rubber Property—Vulcanization Using Oscillating Disk Cure Meter," *Annu. Book ASTM Stand*. **09.01**, 533 (1986).

[21]ASTM Standard D 1485, "Standard Testing Methods for Rubber From Natural Sources—Sampling and Sample Preparation, *Annu. Book ASTM Stand*. **09.01**, 369 (1986).

[22]ASTM Standard D 1456-86, "Standard Test Method for Rubber Property—Elongation at Specific Stress," *Annu. Book ASTM Stand*. **09.01**, 358 (1986).

[23]G. Milani and F. Milani, *Comput. Chem. Eng*., **43**, 173 (2012).

[24]G. Milani, *J. Math. Chem*., **51**, 2038 (2013).

[25]A. I. Isayev and J. S. Deng, RUBBER CHEM. TECHNOL. **61**, 340 (1988).